

<https://helda.helsinki.fi>

Axial dark matter : The case for an invisible Z '

Lebedev, Oleg

2014-06-27

Lebedev , O & Mambrini , Y 2014 , ' Axial dark matter : The case for an invisible Z ' ' ,
Physics Letters B , vol. 734 , pp. 350-353 . <https://doi.org/10.1016/j.physletb.2014.05.025>

<http://hdl.handle.net/10138/217903>

<https://doi.org/10.1016/j.physletb.2014.05.025>

cc_by

publishedVersion

Downloaded from Helda, University of Helsinki institutional repository.

This is an electronic reprint of the original article.

This reprint may differ from the original in pagination and typographic detail.

Please cite the original version.



Axial dark matter: The case for an invisible Z'

Oleg Lebedev^a, Yann Mambrini^{b,*}

^a Department of Physics and Helsinki Institute of Physics, Gustaf Hållströmin katu 2, FIN-00014 University of Helsinki, Finland

^b Laboratoire de Physique Théorique, Université Paris-Sud, F-91405 Orsay, France



ARTICLE INFO

Article history:

Received 24 March 2014

Received in revised form 12 May 2014

Accepted 13 May 2014

Available online 27 May 2014

Editor: A. Ringwald

ABSTRACT

We consider the possibility that fermionic dark matter (DM) interacts with the Standard Model fermions through an axial Z' boson. As long as Z' decays predominantly into dark matter, the relevant LHC bounds are rather loose. Direct dark matter detection does not significantly constrain this scenario either, since dark matter scattering on nuclei is spin-dependent. As a result, for a range of the Z' mass and couplings, the DM annihilation cross section is large enough to be consistent with thermal history of the Universe. In this framework, the thermal WIMP paradigm, which currently finds itself under pressure, is perfectly viable.

© 2014 The Authors. Published by Elsevier B.V. This is an open access article under the CC BY license (<http://creativecommons.org/licenses/by/3.0/>). Funded by SCOAP³.

1. Introduction

Models with an extra U(1) are among the simplest and most natural extensions of the Standard Model (SM). They enjoy both the top-down and the bottom-up motivation. In particular, additional U(1)'s appear in many string constructions. From the low energy perspective, the coupling between an SM fermion f and a massive gauge boson Z' [1]

$$\mathcal{L}_{\text{int}} = g_f Z'_\mu \bar{f} \gamma^\mu (a + b \gamma^5) f, \quad (1)$$

where g_f , a , b are some constants, represents one of the dimension-4 “portals” (see e.g. [2]) connecting the observable world to the SM-singlet sector. This is particularly important in the context of dark matter models [3]. If dark matter is charged under the extra U(1), the above coupling provides a DM annihilation channel into visible particles. As long as the Z' has a TeV scale mass and the couplings are not too small, this framework fits the WIMP-miracle paradigm [4]. Recent LHC [5,6] and direct DM detection constraints [7], however, put significant pressure on this idea since no traces of a Z' were found in either direct collider searches or DM scattering on nuclei.

In this Letter, we argue that these negative results may be due to the axial nature of the Z' and its stronger coupling to dark matter compared to g_f above. In this case, which we call “axial dark matter” (AxDM), DM scattering on nuclei is spin-dependent and weakly constrained. The LHC has limited sensitivity to such a Z' due to the fact that it decays predominantly into dark matter, as

in [8].¹ We thus find that all of the constraints can be satisfied, which adds some credibility to the WIMP paradigm.

2. Axial Z'

In what follows, we consider the possibility that Z' is purely axial, with the couplings²

$$\mathcal{L}_{\text{int}}^{\text{eff}} = \sum_f g_f Z'_\mu \bar{f} \gamma^\mu \gamma^5 f + g_\chi Z'_\mu \bar{\chi} \gamma^\mu \gamma^5 \chi. \quad (2)$$

Here f represents the Standard Model (SM) fermions, χ is a Dirac fermion constituting dark matter and g_f , g_χ are the corresponding Z' couplings. This Lagrangian represents an effective low energy interaction after heavy particles have been integrated out and the vector boson kinetic terms have been diagonalized. Clearly, the microscopic theory can be made anomaly-free by assigning appropriate charges to fermions (we do not exclude the possibility of having further heavy fermions coupled to Z').

One may ask how natural it is to have a pure axial-vector interaction. In our opinion, this choice is quite natural given the fact that the photon interaction is purely vector and the axial case is just the other extreme. Also, our considerations hold in the presence of a small vector component of Z' , which may be generated through kinetic mixing [11].

To make our model as simple as possible, we will focus on the case of a universal coupling of Z' to the SM fermions, g_f .

¹ We allow a Z' to couple universally to SM fermions, which distinguishes the model from the leptophobic scenarios (see e.g. [9]).

² An analysis of the axial DM coupling to the usual Z-boson has recently appeared in [10].

* Corresponding author.

(This assumption can of course be easily relaxed by inserting the fermion-dependent charges.) We then find that cosmological and accelerator constraints require

$$g_f \ll g_\chi, \quad (3)$$

by a factor of $\mathcal{O}(10)$ to $\mathcal{O}(10^3)$. One would be hesitant to attribute such a hierarchy to the difference in the observable and hidden charges. On the other hand, factors of this type can arise in the system of two $U(1)$'s mixing with each other. Consider the general Lagrangian describing two massive abelian gauge bosons,

$$\mathcal{L}_{AB} = -\frac{1}{4}(F_A^{\mu\nu})^2 - \frac{a}{2}F_A^{\mu\nu}F_{B\mu\nu} - \frac{1}{4}(F_B^{\mu\nu})^2 + \frac{1}{2}M_1^2 A_\mu^2 + \delta M^2 A_\mu B^\mu + \frac{1}{2}M_2^2 B_\mu^2, \quad (4)$$

where A couples only to the dark sector with coupling g_A , while B couples only to the visible sector with coupling g_B . The lighter mass eigenstate would be a mixture of A and B , which couples to both sectors. The hierarchy (3) can then be recovered in various limits. For example, it can result from $M_1^2 \ll M_2^2$. For order one kinetic mixing, $a \sim 1$, the Z' is composed mostly of A and

$$g_\chi = \mathcal{O}(g_A), \quad g_f = \mathcal{O}\left(\frac{M_1^2}{M_2^2} g_B\right). \quad (5)$$

Another possibility is to attribute (3) to the hierarchy in the couplings, $g_A \gg g_B$. For a small kinetic mixing $a \sim 0$ and large mass mixing $M_1^2 \sim M_2^2 \sim \delta M^2$, the Z' is a mixture of A and B with

$$g_\chi = \mathcal{O}(g_A), \quad g_f = \mathcal{O}(g_B). \quad (6)$$

Note that for $M_1^2 \approx M_2^2 \approx \delta M^2$, the mixing is nearly maximal and the second mass eigenstate becomes heavy. In what follows, we will be agnostic as to the origin of the hierarchy (3) and will treat the two couplings as free parameters.

3. Dark matter and Z' phenomenology

In this section, we provide a list of cosmological and accelerator constraints on the model. These set bounds on the two couplings g_f , g_χ and the Z' mass $m_{Z'}$. In order to understand their qualitative behaviour and compatibility, we provide simple analytic approximations for the observables.

3.1. Planck/WMAP and DM annihilation

Suppose that DM is produced thermally, as in the traditional WIMP scenario. The main dark matter annihilation mechanism is the s -channel annihilation into SM fermion pairs. Although we will use the exact tree-level result in our numerical analysis, it is instructive to consider the heavy Z' , $m_{Z'}^2 \gg m_\chi^2$, and zero DM-velocity limit.³ In this case, the cross section takes on a particularly simple form,

$$\langle \sigma v \rangle = \frac{g_f^2 g_\chi^2}{2\pi} c_f \sqrt{1 - \frac{m_f^2}{m_\chi^2} \frac{m_f^2}{m_{Z'}^4}}, \quad (7)$$

where c_f is the number of colors for quarks and 1 for leptons. We see that, for light final state fermions, the cross section is suppressed. The origin of the $m_f^2/m_{Z'}^2$ factor can be understood from

(conserved) C-parity considerations. The C-parity of the initial state must be $+1$ to match that of Z' . Since for a fermion–antifermion pair it is given by $(-1)^{l+s}$ with l and s being the angular momentum and spin quantum numbers, the s -wave initial state ($v \rightarrow 0$) must then have $s = 0$. On the other hand, the helicities of the relativistic final state fermions add up to 1. Hence, a spin flip is required leading to the $m_f/m_{Z'}$ dependence. Note however that, for heavy fermions like the top quark, this factor does not lead to significant suppression of the amplitude.

Suppose that DM is sufficiently heavy such that its pair annihilation into top quarks is allowed. Then for $\sqrt{1 - m_t^2/m_\chi^2} \sim 1$, the canonical WIMP annihilation cross section $\sigma v = 3 \times 10^{-26} \text{ cm}^3 \text{ s}^{-1}$ translates into

$$\frac{m_{Z'}}{\sqrt{g_f g_\chi}} \sim 1500 \text{ GeV}. \quad (8)$$

One should keep in mind that this figure indicates the ballpark of the result and the velocity- as well as m_χ -dependent contributions affect $\langle \sigma v \rangle$, while the definitive answer is given by our numerical analysis.

3.2. Direct DM detection

Tree level Z' exchange leads to spin-dependent DM scattering on nuclei, which is constrained by a number of experiments. For an (approximately) universal Z' coupling to quarks,

$$\sigma^{\text{SD}} = \frac{12 g_f^2 g_\chi^2 m_N^2}{\pi m_{Z'}^4} (\Delta_u + \Delta_d + \Delta_s)^2, \quad (9)$$

where m_N is the nucleon mass and Δ_i are the quark contributions to the proton spin: $\Delta_u = 0.84$, $\Delta_d = -0.43$, $\Delta_s = -0.09$. Taking 10^{-39} cm^2 as the benchmark bound on σ^{SD} for $m_\chi \sim 100 \text{ GeV}$ [12], one finds

$$\frac{m_{Z'}}{\sqrt{g_f g_\chi}} > 600 \text{ GeV}. \quad (10)$$

This bound is satisfied automatically for thermally produced dark matter (see Eq. (8)). The crucial factor is that the coupling to visible matter is axial, while that to DM could in principle contain a vector component.

Spin-independent DM scattering is generated at one loop with the corresponding amplitude being suppressed both by a loop factor and the quark masses required by a helicity flip. The resulting bound is weak [13].

We note that similar conclusions apply to the DM–nucleon interaction mediated by a pseudoscalar as recently studied in [14].

3.3. LEP bounds

Dark matter with $m_\chi > m_t$ cannot be produced on-shell at LEP. However, there are still significant constraints on Z' due to the effective operators

$$\frac{g_f^2}{m_{Z'}^2} \bar{f}_i \gamma^\mu \gamma^5 f_i \bar{f}_j \gamma_\mu \gamma^5 f_j, \quad (11)$$

for various fermions f_i and f_j . These operators are constrained by the precise measurements of the cross sections and angular distributions of the final state fermions. In the axial case, the resulting bound is [15]

$$\frac{m_{Z'}}{g_f} > 5 \text{ TeV}. \quad (12)$$

³ Numerically, the velocity-independent terms dominate at relatively low $m_{Z'}$, while for a heavier Z' velocity-dependent contributions are equally important. We choose the limit $v \rightarrow 0$ for transparency of our discussion, while using the full result in our numerical analysis.

Comparing this to Eq. (8), one finds that Z' couples much stronger to DM than it does to SM fermions,

$$\alpha = g_\chi/g_f > 10. \quad (13)$$

3.4. Perturbativity

As is clear from the above discussion, the DM- Z' coupling can become quite strong. Then, our approximation is controllable only if

$$\frac{g_\chi^2}{4\pi^2} < 1. \quad (14)$$

We do not impose further constraints on the position of the Landau pole of the coupling as we expect our model to be UV-completed already in the multi-TeV range.

3.5. Dilepton and monojet LHC bounds

At the LHC, both dark matter and Z' can be produced on-shell, which leads to strong bounds from CMS and ATLAS. The most important constraint is due to searches for dileptons with a large invariant mass. We will use the CMS Z' analysis of $3.6 \text{ fb}^{-1}/8 \text{ TeV}$ and $5 \text{ fb}^{-1}/7 \text{ TeV}$ [5] as our benchmark constraint. The result is summarized in Fig. 2 (upper right panel) of that paper. For a sequential SM Z' (SSM), that is having the same couplings as the Standard Model Z-boson, the exclusion limit is around 2.5 TeV. To adapt the results to our case, one must take into account the difference in the Z' couplings as well as the reduced branching ratio for Z' decay into visible fermions,

$$\sigma_{l^+l^-} \rightarrow \left(\frac{g_f}{g_Z}\right)^2 \text{BR}_{\text{vis}} \sigma_{l^+l^-} \quad (15)$$

For our estimates it suffices to approximate g_Z by its (universal) axial component, $g_Z/(4\cos\theta_W)$. The branching ratio for Z' decay into SM fermions is

$$\text{BR}_{\text{vis}} \simeq \frac{45g_f^2}{45g_f^2 + g_\chi^2\beta^3}, \quad (16)$$

where $\beta = \sqrt{1 - 4m_\chi^2/m_{Z'}^2}$, accounts for the kinematic suppression in an axial-vector decay (see e.g. [16]). These factors result in the dependence of the number of expected l^+l^- events on g_f and g_χ . The constraints on Z' relax significantly as g_f decreases and $m_{Z'}$ as light as 500 GeV becomes allowed given it decays predominantly invisibly.

To estimate the resulting LHC bound on $m_{Z'}$, we analytically approximate the l^+l^- production cross section in Fig. 2 of [5] and calculate how much it should be reduced to comply with its experimental bound. We find that the result can be cast in the form $m_{Z'} > m_0 + 0.55 \log_{10}[(g_f/0.17)^2 \text{BR}_{\text{vis}}]$, for $m_{Z'}$ in TeV and m_0 being an $m_{Z'}$ -range dependent constant: $m_0 \simeq (2, 2.3, 2.5) \text{ TeV}$ for $m_{Z'} \sim (0.5, 1, \geq 1.5) \text{ TeV}$. For instance, a 500 GeV Z' becomes allowed if the l^+l^- cross section reduces by about 3 orders of magnitude, whereas a 2.5 TeV Z' is allowed with no suppression required.

Z' models are also constrained by monojet events with large missing energy, which is due to Z' decay into dark matter. The ATLAS analysis of $10.5 \text{ fb}^{-1}/8 \text{ TeV}$ data [17] imposes the bound on the axial-vector interaction (D8-operator of [18]),

$$\frac{m_{Z'}}{\sqrt{g_f g_\chi}} > 600\text{--}700 \text{ GeV}, \quad (17)$$

for $m_\chi \sim 200 \text{ GeV}$ (and a weaker bound for heavier DM). Inclusion of on-shell effects does not make the constraint significantly stronger [8]. As a result, similarly to the direct DM detection constraint, it is satisfied when Eq. (8) is imposed.

3.6. Combined constraints

The above estimates serve to single out the most important constraints, whose compatibility is to be analyzed. We see that, once the correct DM relic abundance is imposed, the main factors restricting available parameter space are the LHC dilepton bound and perturbativity. Indeed, the LHC constraint can always be satisfied by decreasing g_f , which according to Eq. (8) increases g_χ until it hits the perturbative bound (14). We find that all of the constraints are in fact compatible. For instance, at $m_{Z'} \sim 500 \text{ GeV}$, the allowed range of $\alpha = g_\chi/g_f$ spans about two orders of magnitude, from $\mathcal{O}(10)$ to $\mathcal{O}(10^3)$.

To go further, let us remind the reader that our estimate of the DM relic abundance constraint (8) is rather simplistic. It does not take into account resonant effects nor those due to thermal averaging. The correct treatment is provided by the numerical package micrOMEGAs [19]. Using this tool, we find the same qualitative conclusion: all of the constraints are compatible. In our numerical study, we impose the condition⁴

$$m_{Z'} > 2m_\chi, \quad (18)$$

which allows for the Z' decay into dark matter and amounts to “invisibility” of the former. Two representative results are shown in Fig. 1. In the left panel, we set $m_\chi = 250 \text{ GeV}$, $g_f = 0.005$ and scan parameter space $\{m_{Z'}, g_\chi\}$ satisfying the PLANCK constraint [20]. As $m_{Z'}$ increases from $2m_\chi$, so does g_χ . In this region, the effect of resonant annihilation is important. The resonance is quite broad, on the order of tens of GeV, due to the thermal smearing. Away from the resonance, g_χ quickly turns non-perturbative. The LHC constraint excludes part of the parameter space close to the threshold, where the invisible Z' decay is inefficient. Further constraints from LEP, direct DM detection and monojets are satisfied automatically in this panel. The result is that the $m_{Z'}$ range 520–560 GeV is allowed, while g_χ varies by two orders of magnitude, from 0.05 to 5.

For heavier DM, the LHC bound becomes less severe and the coupling g_f is allowed to be larger. For example, in the right panel of Fig. 1, the CMS constraint is satisfied everywhere due to the suppressed Z' production with $g_f = 0.05$. The $m_{Z'}$ range satisfying PLANCK extends over hundreds of GeV.

The pattern observed in this figure is quite general: the allowed parameter space is not far from the resonance region, $m_{Z'} \gtrsim 2m_\chi$, with the latter being relatively broad, $\sim 10\text{--}20\%$ $m_{Z'}$. The LEP, direct DM detection and monojet constraints are satisfied automatically in the region of interest, while the dilepton LHC bound cuts out part of the parameter space. The dark matter candidate, AxDM, belongs to the general WIMP category as it has a TeV scale mass and couplings in the range $\mathcal{O}(10^{-2}\text{--}1)$. A detailed scan of AxDM parameter space is reserved for a subsequent publication.

4. Conclusion

In this paper, we have explored a very simple scenario in which dark matter couples to the SM fermions via an axial Z' (“axial dark matter”). The model is characterized by 2 couplings as well as the

⁴ This condition may not be necessary if the coupling g_f is very small and the Z' production cross section is suppressed altogether.

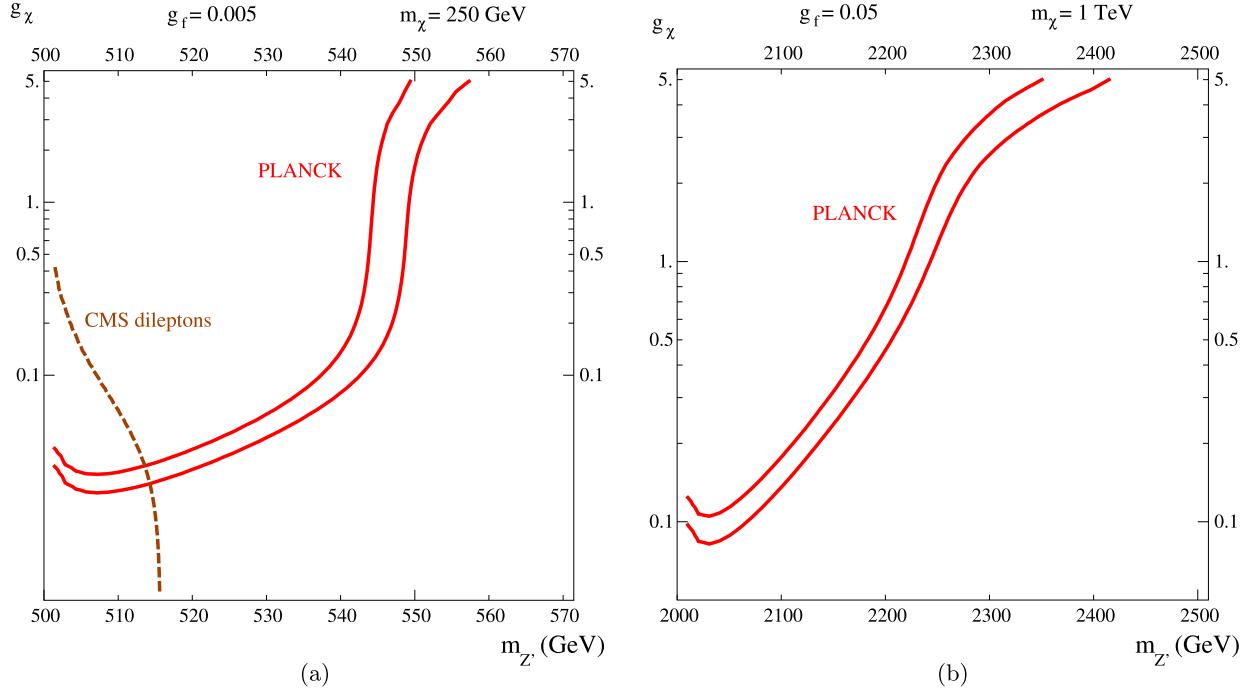


Fig. 1. Relic density (Planck) and direct search (CMS dileptons) constraints on Z' for lighter (left panel) and heavier (right panel) dark matter. The area between the two red (solid) lines is consistent with Planck, while the area below the brown (dashed) line is excluded by CMS. Other constraints (LEP, direct DM detection, monojets) are satisfied automatically.

Z' and DM masses. If the Z' couples much stronger to the dark sector compared to the visible sector, which may be due to a mixing of two $U(1)$'s, all the phenomenological constraints can be satisfied. In particular, the LHC constraints are loose due to invisible Z' decay and allow for $m_{Z'}$ as low as 500 GeV, while DM scattering on nuclei is spin-dependent and thus weakly constrained. The correct DM relic density is obtained in regions not far from the resonance, $m_{Z'} \gtrsim 2m_\chi$. All in all, we find that AxDM is consistent with the thermal WIMP paradigm.

Acknowledgements

The authors would like to thank G. Arcadi, B. Zaldivar, M. Tytgat and K. Tarachenko for very useful discussions. This work was supported by the French ANR TAPDMS ANR-09-JCJC-0146 and the Spanish MICINN's Consolider-Ingenio 2010 Programme under grant Multi-Dark CSD2009-00064. Y.M. acknowledges partial support from the European Commission FP7 ITN INVISIBLES (Marie Curie Actions, PITN-GA-2011-289442) and from the ERC Advanced Grant Higgs@LHC 321133.

References

- [1] P. Langacker, *Rev. Mod. Phys.* **81** (2008) 1199; T. Han, P. Langacker, Z. Liu, L.-T. Wang, arXiv:1308.2738 [hep-ph].
- [2] F. Domingo, O. Lebedev, Y. Mambrini, Jérém Quevillon, A. Ringwald, *J. High Energy Phys.* **1309** (2013) 020.
- [3] K. Cheung, T.-C. Yuan, *J. High Energy Phys.* **0703** (2007) 120; Y. Mambrini, *J. Cosmol. Astropart. Phys.* **1107** (2011) 009; V. Barger, D. Marfatia, A. Peterson, *Phys. Rev. D* **87** (2013) 015026; E. Dudas, L. Heurtier, Y. Mambrini, B. Zaldivar, *J. High Energy Phys.* **1311** (2013) 083.
- [4] G. Bertone, D. Hooper, J. Silk, *Phys. Rep.* **405** (2005) 279.
- [5] CMS Collaboration, S. Chatrchyan, et al., *Phys. Lett. B* **720** (2013) 63.
- [6] ATLAS Collaboration, G. Aad, et al., *J. High Energy Phys.* **1211** (2012) 138.
- [7] LUX Collaboration, D.S. Akerib, et al., arXiv:1310.8214 [astro-ph.CO].
- [8] G. Arcadi, Y. Mambrini, M.H.G. Tytgat, B. Zaldivar, arXiv:1401.0221 [hep-ph].
- [9] A. Alves, S. Profumo, F.S. Queiroz, arXiv:1312.5281 [hep-ph].
- [10] A. De Simone, G.F. Giudice, A. Strumia, arXiv:1402.6287 [hep-ph].
- [11] B. Holdom, *Phys. Lett. B* **166** (1986) 196.
- [12] XENON100 Collaboration, E. Aprile, et al., *Phys. Rev. Lett.* **111** (2) (2013) 021301; PICASSO Collaboration, S. Archambault, et al., *Phys. Lett. B* **711** (2012) 153; COUPP Collaboration, E. Behnke, et al., *Phys. Rev. D* **86** (2012) 052001.
- [13] M. Freytsis, Z. Ligeti, *Phys. Rev. D* **83** (2011) 115009.
- [14] C. Boehm, M.J. Dolan, C. McCabe, M. Spannowsky, C.J. Wallace, arXiv:1401.6458 [hep-ph].
- [15] ALEPH and DELPHI and L3 and OPAL and LEP Electroweak Working Group Collaborations, J. Alcaraz, et al., arXiv:hep-ex/0612034.
- [16] S. Heinemeyer, W. Hollik, A.M. Weber, G. Weiglein, *J. High Energy Phys.* **0804** (2008) 039.
- [17] ATLAS Collaboration, Search for new phenomena in monojet plus missing transverse momentum final states using 10 fb^{-1} of pp Collisions, at $\sqrt{s} = 8 \text{ TeV}$ with the ATLAS detector at the LHC, ATLAS-CONF-2012-147.
- [18] J. Goodman, M. Ibe, A. Rajaraman, W. Shepherd, T.M.P. Tait, H.-B. Yu, *Phys. Rev. D* **82** (2010) 116010.
- [19] G. Belanger, F. Boudjema, A. Pukhov, A. Semenov, *Comput. Phys. Commun.* **185** (2014) 960.
- [20] P.A.R. Ade, et al., Planck Collaboration, arXiv:1303.5062 [astro-ph.CO].